J Mater Sci (2011) 46:5916–5924
DOI 10.1007/s10853-011-5545-1

Variation of solute distributions during deformation and bake hardening process and their effect on bake hardening phenomenon in ultra-low carbon bake hardening steels

Hua Wang · Wen Shi · Yan Lin He · Peng Peng Liu · Lin Li

Received: 23 December 2010 / Accepted: 6 April 2011 / Published online: 20 April 2011
© Springer Science+Business Media, LLC 2011

Abstract Three-dimensional atom probe was used to investigate solute carbon and other elements distributions during bake hardening process after pre-deformation and also to analyze their effect on bake hardening phenomenon of the steels. Two different kinds of bake hardening steels were prepared and annealed by water quenching. The as-received samples were pre-deformed at different levels (from 0 to 10%), and baked at 170 °C for 20 min. Distributions and concentrations of solute elements in the steels were characterized with three-dimensional atom probe. Bake hardening values of the steels were examined by tensile experiments. Three dimensional atom probe detection results indicate that C distribution changes little with the increase of pre-deformation in BH-Mn steel. In BH-P steel, however, with the increase of pre-deformation, more C clusters form in the matrix and C concentration decreases. Distribution patterns and the maximum separation distance method results prove that the C cluster is just C segregation or C together with P segregation rather than vanadium carbides precipitate. Moreover, bake hardening experiment results indicate that BH values are similar in the two BH steels and the BH values change only a little as the pre-deformation increases from 2 to 10%. The 4% pre-deformation induces the highest BH values in the two BH steels, and is considered to be the critical pre-deformation in making the balance of Cottrell atmosphere in the two BH steels.

Introduction

Various types of bake hardening (BH) steels have been developed very quickly due to their excellent properties as automotive body panel since 1981 [1]. BH steel, which is developed from interstitial free (IF) steel, is similar to IF steel with good deep drawing property. However, the strengths of BH and IF steels are quite different from each other since BH steel has BH property. BH is one of the most important properties for BH steel. BH value is generally affected by the interaction between solute C and dislocations.

A number of investigations have been published on BH phenomenon of BH steels [2–6], and most of them focused on the concentration of solute C using internal friction value [7–10], based on the relationship between the concentration of solute C and BH value. For example, De Cooman and co-workers [8] obtained the changing law of solute C concentration in BH steels with two different pre-deformation by internal friction method. However, internal friction experiment cannot obtain solute C distribution pattern and its effect on BH value.

Three-dimensional atom probe (3DAP) can diagnose solute element atoms as well as nano-sized precipitates, and this method also can quantify solute segregation at precipitate–matrix interfaces of precipitates as small as 2-nm in diameter [11]. A number of studies have successfully applied 3DAP in detecting solute elements as

H. Wang · W. Shi · Y. L. He · P. P. Liu · L. Li
College of Materials Science and Engineering, Shanghai University, Shanghai 200072, China

H. Wang (✉)
Shanghai University, Room 403, Metal Building, No. 149, Yanchang Road, Shanghai 200072, China
e-mail: hwang225@gmail.com

well as precipitates [12–20]. For example, Hono and co-workers [17] used 3DAP to detect the solute elements in an age-hardened Mg–Ca–Zn alloy. They obtained the distribution patterns of the observed elements.

In the current study, 3DAP was employed to detect the solute distributions in the matrix of the two annealed steels and also the baked steels with different pre-deformations (2 and 6%). Tensile experiments were carried out to measure BH values of the pre-deformed steels. The relationship between C distributions and concentrations and BH phenomenon was discussed experimentally.

Experimental procedure

Ultra-low carbon bake hardening (ULC-BH) steels (BH-Mn and BH-P) specimens were prepared with different contents of P and Mn, and the contents of V and other elements had no significant difference. BH-Mn steel was prepared with 1.44 wt% Mn but a quite small amount of P, and BH-P steel with 0.054 wt% P and a quite small amount of Mn. The detailed chemical compositions of the two raw steels and the annealed and deformed steels are given in Table 1.

For the raw steels elements detection, the carbon was determined by Leco Carbon/Sulfur Analyzer, the N element was determined by Leco Nitrogen/Oxygen Determinator, and the other elements were determined by Inductively Coupled Plasma-Atomic Emission Spectroscopy (ICP-AES).

The atom concentrations in annealed and deformed steels were detected using 3DAP and shown by a data range according to the composition profiles obtained from 3DAP results. The concentration of solute element is calculated from the 3DAP detection composition profiles, and the equation is as follows:

$$C\,\mathrm{wt}\% = \frac{C\,\mathrm{at}\% \times \mathrm{Ar}_c}{\sum_i X_i\,\mathrm{at}\% \times \mathrm{Ar}_{X_i}} \quad (1)$$

where wt% is the mass fraction, at% is the atom number fraction, Ar is the relative atom mass, X_i is the element in the matrix, and the elements with very little content are neglected during the calculation.

The sample preparation process was as follows: (1) Steel was melted in a vacuum induction furnace and poured into a spindle; (2) Solidified steel was forged into 25-mm thick flats; (3) The thick steel flats were hot rolled into 4.5 mm strips in thickness with a finishing rolling temperature of 930 °C and then used air-cool; (4) The obtained 4.5 mm strips were further cold rolled to steel sheets with thickness of 0.8 mm, then treated in a salt bath furnace at 800 °C for 2 min, and finally cooled by water quenching.

For 3DAP analysis [21–24], an Oxford nanoScience energy-compensated 3DAP field ion microscope was used under ultrahigh vacuum conditions ($<10^{-10}$ mbar). Specimens were cooled to −193 °C during testing process, the frequency of pulse voltage was 2 kHz, the pulse fraction was 20%, and the detector efficiency was 45%. The specimens for atom probe test were first prepared by square bars with dimensions of 0.5 × 0.5 × 50 mm^3, and then electro-polished by two steps using a 25% perchloric acid–75% acetic acid solution for stage one and a 2% perchloric acid–98% ethylene glycol monobutyl ether solution for stage two. The final specimens for testing were sharp needle-like columns. The testing results were analyzed by Posap software [25]. Various values were tested for the commonly used particle analysis parameters—maximum distance between solute atoms ($D_{\max} = 0.8$), surround distance ($L = 0.8$), erosion distance ($S = 0.8$), and the minimum number of detected solute atoms comprising an aggregate ($N_{\min} = 8$).

In order to examine BH values of the investigated BH steels, specimens were pre-deformed by different pre-deformations (from 0 to 10%) and aged at 170 °C for 20 min, which were further re-stretched to rupture. Specimens were prepared according to ASTM E8/E8M-09 standards.

Table 1 Chemical composition of the test steels (wt%)

Steels	C	N	Mn	S	Si	P	Al	V	Ti
BH-Mn	0.0123	0.0057	1.44	0.011	0.064	0.009	0.061	0.090	0.013
Annealed	0.006–0.017		0.295–1.67		0.02–0.045	0.022–0.05	0.039–0.138	0.027–0.064	
2% pre-deformed	0.009–0.018		0.246–0.786		0.02–0.04	0.017–0.039	0.039–0.169	0.055–0.128	
6% pre-deformed	0.009–0.017		0.226–0.884		0.02–0.04	0.028–0.055	0.043–0.149	0.036–0.082	
BH-P	0.0137	0.003	0.07	0.008	0.036	0.054	0.12	0.090	0.021
Annealed	0.011–0.03		0.098–0.31		0.02–0.1	0.055–0.22	0.048–0.15	0.036–0.13	
2% pre-deformed	0.004–0.01		0.029–0.049		0.025–0.055	0.033–0.133	0.053–0.166	0.046–0.1	
6% pre-deformed	0.002–0.006		0.02–0.059		0.015–0.03	0.017–0.083	0.043–0.13	0.046–0.082	

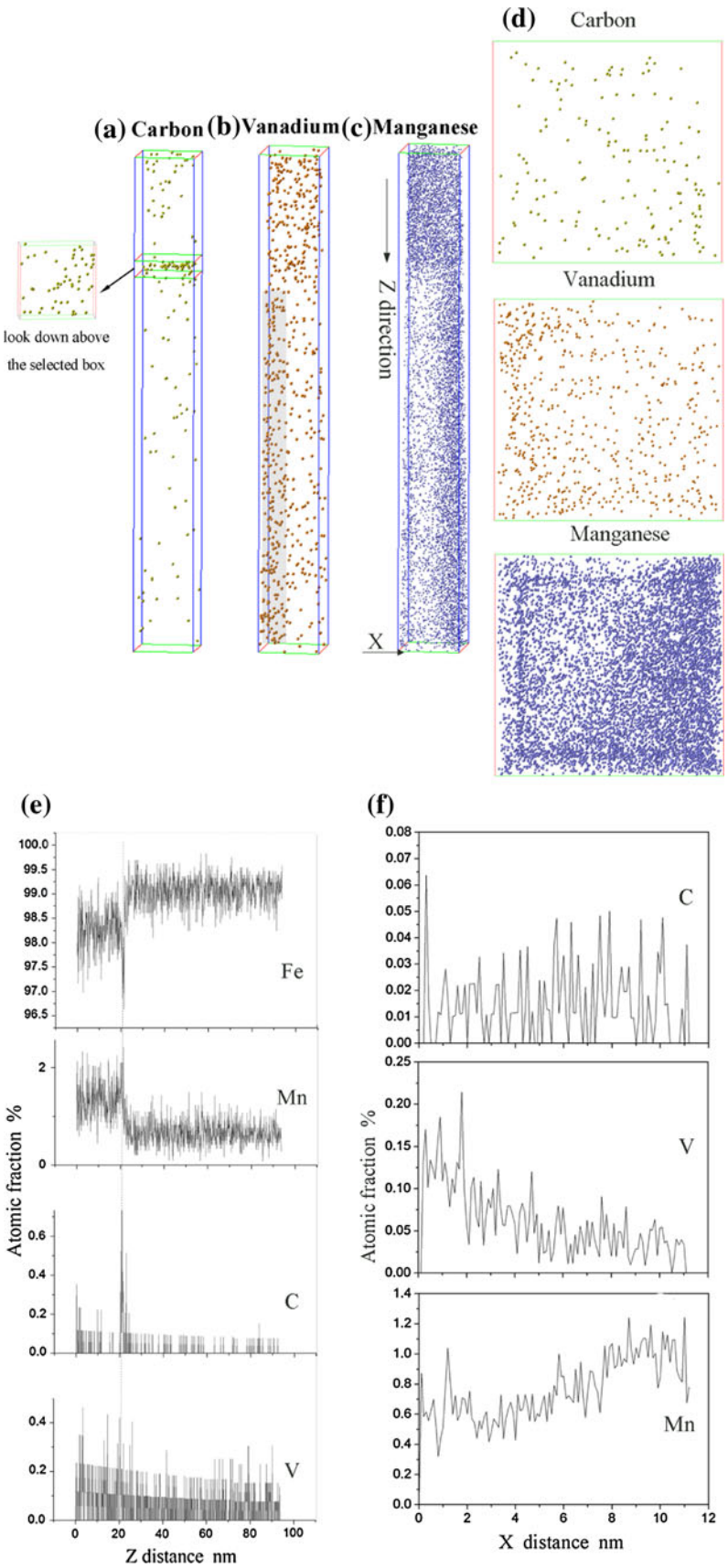

Fig. 1 3DAP measured distributions of C (**a**), V (**b**), Mn (**c**) in length and these atoms (**d**) in transverse section of observed area in BH-Mn steel and its composition profiles in *Z* direction (**e**) and *X* direction (**f**) (box size: 11 × 11.3 × 93.8 nm)

Results and discussions

Solute distributions in annealed BH steels

Solute distributions in the two annealed steels and the hot-rolled BH-Mn steel are shown in Figs. 1, 2, and 3.

Figure 1 shows the distribution patterns and concentrations of solute elements in annealed BH-Mn steel detected by 3DAP. This result has also been mentioned in another article [26]. C is segregated in the area of selected box (see Fig. 1a), but no V and Mn segregations were found in the selected box area (see Fig. 1b–d). That is, the segregated C exists as segregation rather than forms vanadium carbides during the continuous annealing process, and this conclusion has also been confirmed by Soene et al. [9]. The distribution patterns of Mn vary in C cluster of selected box area, as shown in Fig. 1c and d. The C cluster area is grain boundary or Cottrell atmosphere, which can not be determined clearly. V shows a little segregation (see Fig. 1b and f), and the V segregation area is just different from the Mn segregation area (see Fig. 1c and f).

Figure 2 shows the solute distributions in hot-rolled BH-Mn steel, which indicates that there is C and V cluster in the steel matrix. Comparing the results in Fig. 2 with Fig. 1, it can be concluded that vanadium carbides are dissolved and form solute C which segregates in grain boundaries or dislocations during the annealing process.

The concentrations of solute C and V in annealed BH-Mn steel can be calculated using 3DAP results (Fig. 1d). The concentrations of solute C and V are 0.006–0.017 wt% (a concentration range calculated from the 3DAP composition profile) and 0.027–0.064 wt%, respectively, as listed in Table 1.

Solute distributions in annealed BH-P steel are shown in Fig. 3. The results (Fig. 3) show that C distributes homogeneously in the steel matrix, V shows almost no segregation, whereas P segregates in the steel matrix. The concentration of solute C and V is 0.011–0.03 wt% and 0.036–0.13 wt%, respectively, as listed in Table 1. From the solute distributions in the two annealed BH steels as shown in Figs. 1 and 3 and the solute concentrations shown in Table 1, it can be concluded that C concentration in

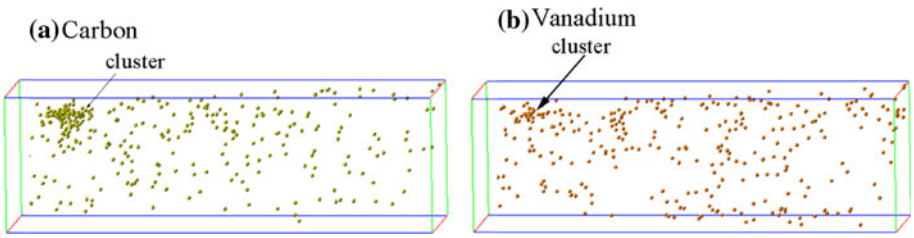

Fig. 2 3DAP measured cluster of C (**a**) and V (**b**) in hot-rolled BH-Mn steel (box size: 14 × 14.4 × 42.6 nm)

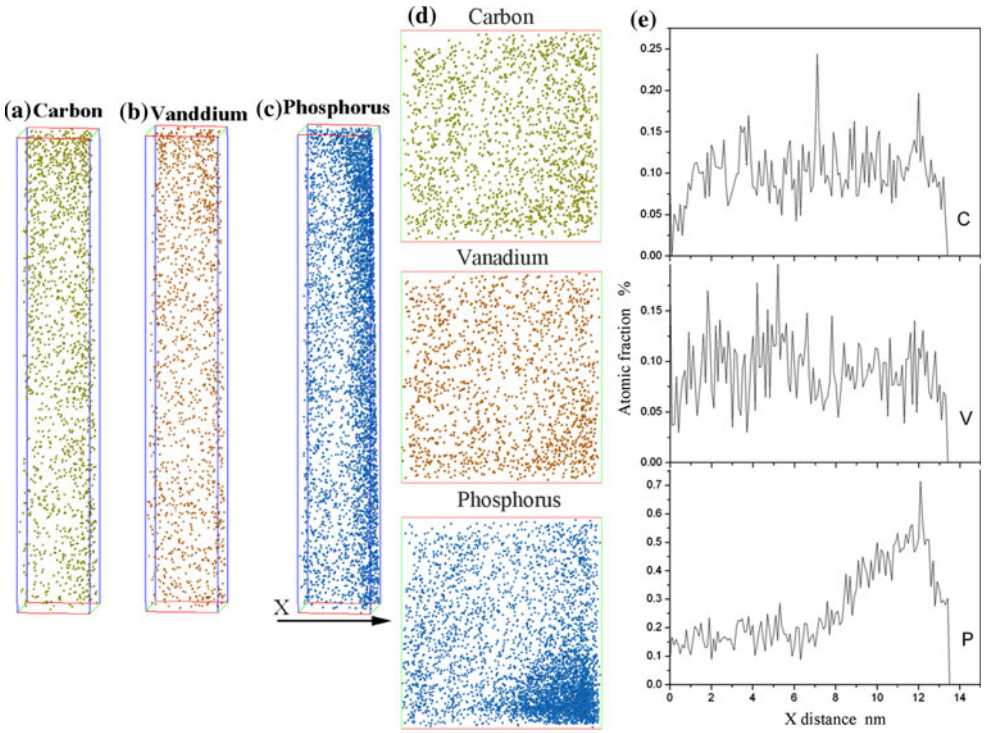

Fig. 3 3DAP measured distributions of C (**a**), V (**b**), P (**c**) in length and these atoms (**d**) in transverse section of observed area in annealed BH-P steel and its composition profile in *X* direction (**e**) (box size: 13.6 × 14.4 × 87 nm)

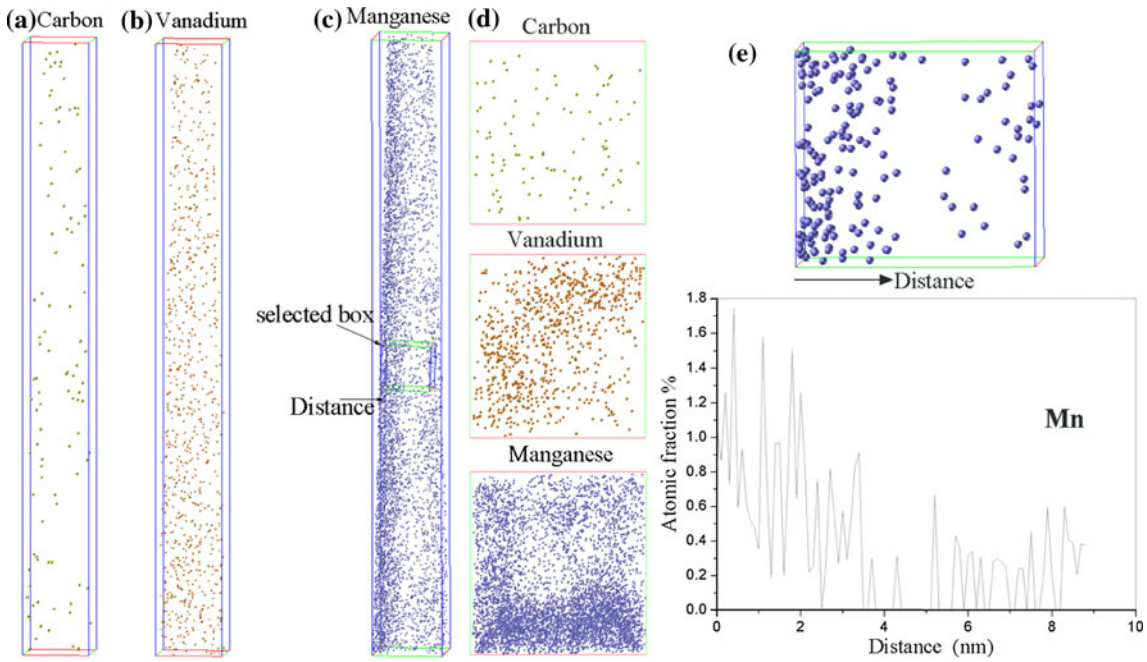

Fig. 4 3DAP measured distributions of C (**a**), V (**b**), Mn (**c**) in length and these atoms (**d**) in transverse section of observed area in 2% pre-deformed BH-Mn steel and Mn distribution and atomic fraction in the selected box (**e**) (the bar box size: 12 × 12.5 × 110.7 nm)

annealed BH-P steel is obviously higher than that in BH-Mn steel.

In both BH steels, there is no dissolved N element. It can be concluded that BH phenomenon is mainly induced by C element pinning the dislocations in the investigated steels.

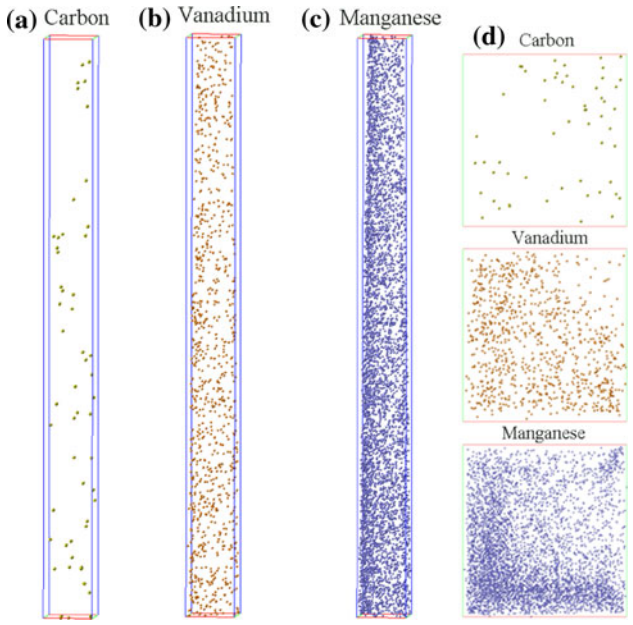

Fig. 5 3DAP measured distributions of C (**a**), V (**b**), Mn (**c**) in length and these atoms (**d**) in transverse section of observed area in 6% pre-deformed BH-Mn steel (box size: 10 × 10.5 × 119 nm)

Solute distributions in pre-deformed and baked BH-Mn steel

Figure 4 shows solute distributions in baked BH-Mn steel after 2% pre-deformation. As shown in Fig. 4, there are very few scattered C atoms in the matrix. The C concentration is as low as 0.009–0.018 wt% (see Table 1), which is similar to that in annealed BH-Mn steel. As investigated by De Cooman and co-workers with static analysis [8, 27, 28], C will diffuse into grain boundaries and dislocations during the baking process. However, C changes little in the BH-Mn steel during the pre-deformation and baking process. This is possibly due to the reason that the solute C in the BH-Mn steel matrix is too few to diffuse. There is obvious V segregation in the matrix. The solute V concentration is approximately 0.055–0.128 wt% (see Table 1). Since the V exists as segregation, V concentration in the 2% deformed BH-Mn steel is higher than that in the annealed one (see Figs. 1 and 4 and Table 1). Mn segregates in the matrix (see Fig. 4), but the Mn segregation area is different from V segregation. The segregation of Mn is considered to be dislocations or the Ferrite grain boundary segregation since there is only Ferrite phase in the investigated steel.

Figure 5 shows solute distributions in 6% pre-deformed BH-Mn steel detected by 3DAP. There are only a few C atoms scattered in the matrix (Fig. 5a), and the concentration of C is 0.009–0.017 wt% according to Table 1,

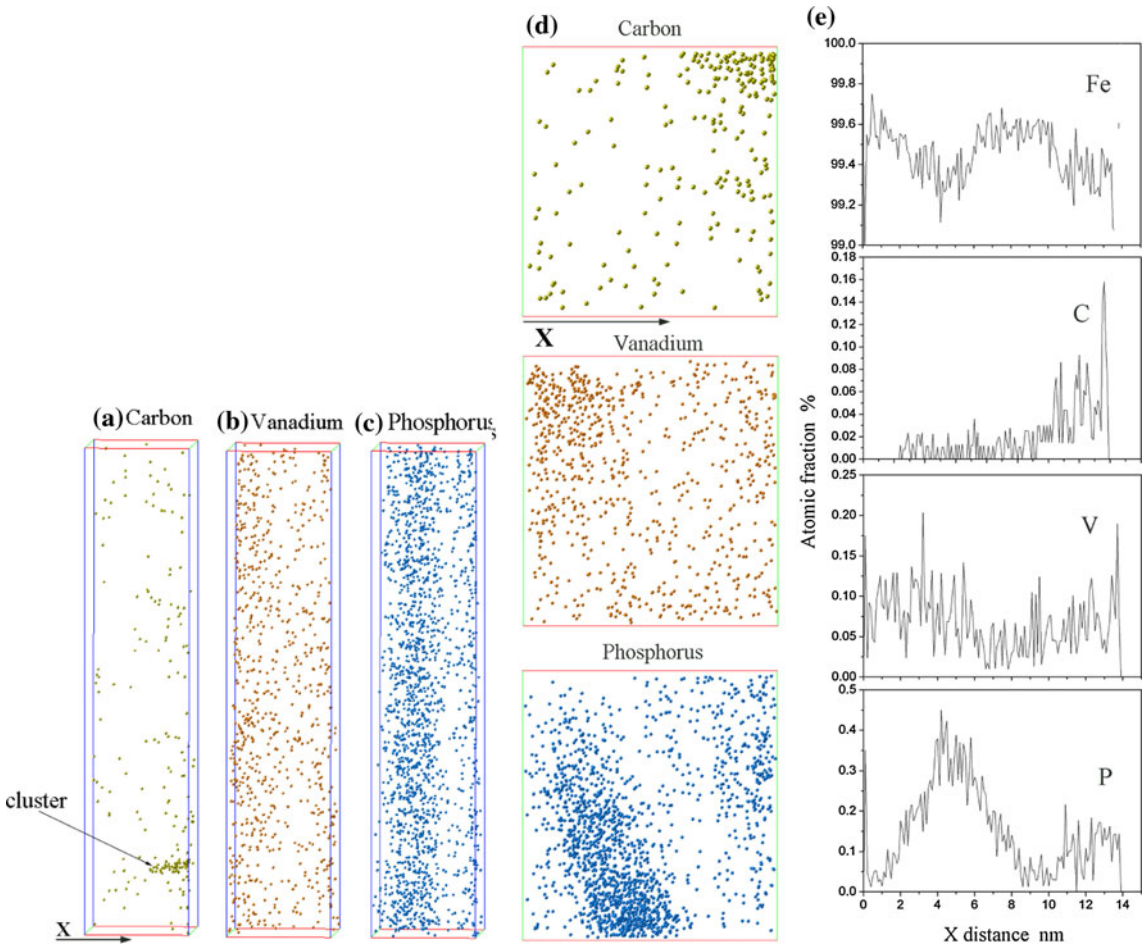

Fig. 6 3DAP measured distributions of C (**a**), V (**b**), P (**c**) in length and these atoms (**d**) in transverse section of observed area in 2% pre-deformed BH-P steel and its composition profiles in *X* direction (**e**) (box size: 14 × 14.8 × 65 nm)

which is similar to that in 2% pre-deformed BH-Mn steel. Different from the 2% pre-deformed BH-Mn steel, however, the V in 6% pre-deformed BH-Mn steel distributes almost homogeneously in the matrix, and the concentration of it is 0.036–0.082 wt% (see Table 1). Mn segregates obviously in the steel matrix (Fig. 5), similar to that in the 2% pre-deformed BH-Mn steel.

Solute distributions in pre-deformed and baked BH-P steel

Solute distributions characterized by 3DAP in 2% pre-deformed BH-P steel are shown in Fig. 6. From Fig. 6a and d, it is seen that some C clusters exist in the matrix, which is different from that in the annealed BH-P steel (Fig. 3). It can be concluded that solute C diffuses and forms clusters during the baking process after pre-deformation. According to Table 1, C concentration in the 2% pre-deformed and baked BH-P steel is 0.004–0.01 wt%, much less than that of the annealed one. This is in agreement with the discussions in "Solute distributions in pre-deformed and baked BH-Mn steel" section that C diffuses to grain boundaries and dislocations during the baking process after pre-deformation, and makes the decrease of C concentration in the matrix.

V also shows segregation (Fig. 6b), but the V segregation area is quite different from C cluster area (Fig. 6a). So the C cluster is a C collection rather than vanadium carbide precipitate. P exists as segregation, the same to that in the annealed one. From Fig. 6d and e, it can be seen that V segregation area is just different from the P segregation.

Solute distributions of 6% pre-deformed BH-P steel are shown in Fig. 7. It is found that more C clusters are formed in this steel than the 2% pre-deformed one. The concentration of C in the matrix is 0.002–0.006 wt% (see Table 1), a little lower than the 2% pre-deformed one. The result that more C clusters and lower C concentration in matrix of the 6% pre-deformed BH-P steel than the 2% pre-deformed one indicates that there is more C diffuses and segregates when the pre-deformation increases. V distributes homogeneously in the matrix. So the C clusters are C segregations rather than the vanadium carbides

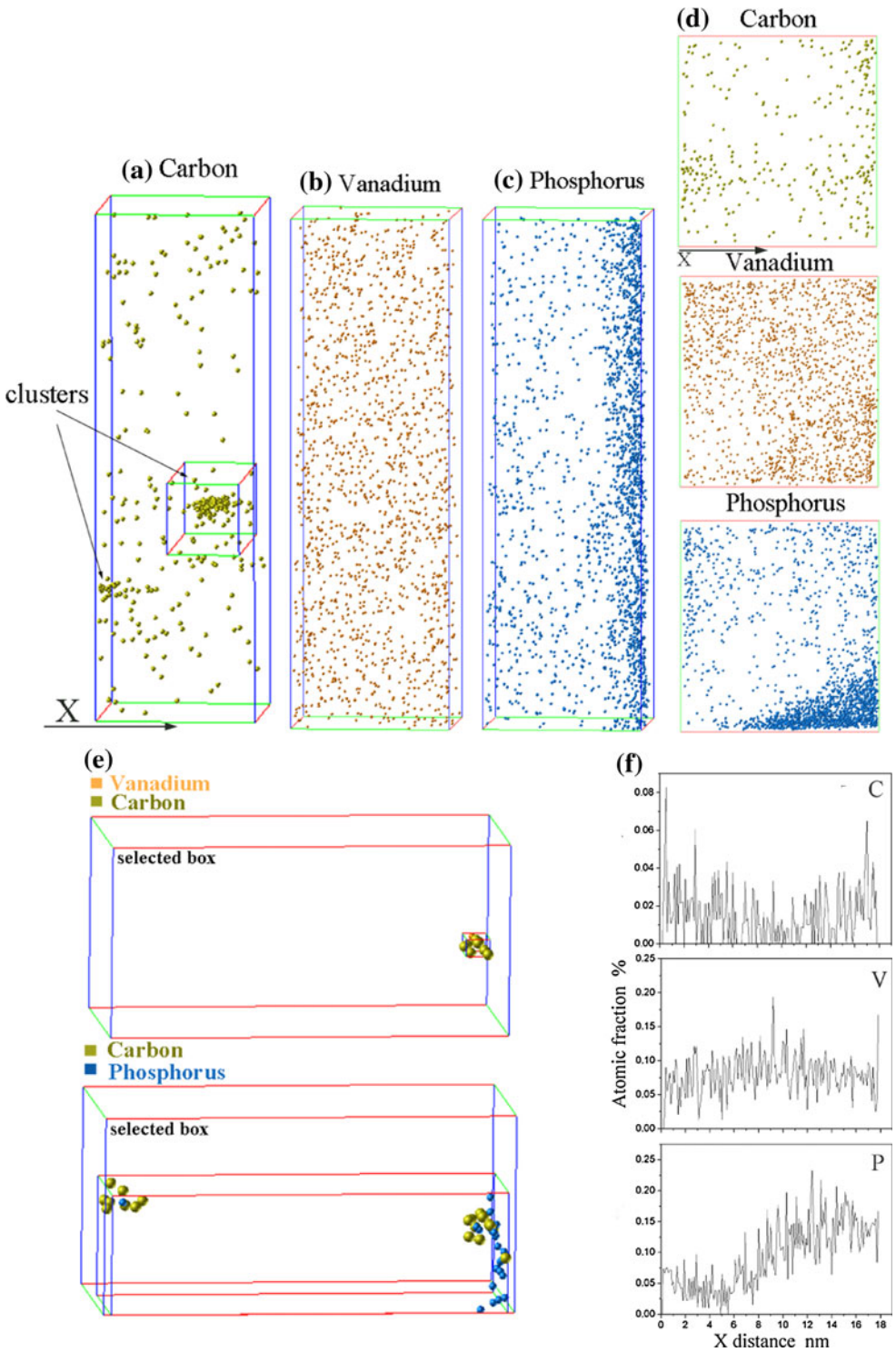

Fig. 7 3DAP measured distributions of C (**a**), V (**b**), P (**c**) in length and these atoms (**d**) in transverse section of observed area and C clusters (**e**) examined by maximum separation distance method in 6% pre-deformed BH-P steel and its composition profile in *X* direction (**f**) (box size: 18 × 19 × 61 nm)

precipitates. In order to prove this result, the maximum separation distance method was used to detect the C cluster as shown in Fig. 7e. It can be seen that the C cluster contain almost no V atoms but many P atoms. So, the C actually segregates together with P in the 6% pre-deformed BH-P steel.

BH phenomenon in the two BH steels

Figure 8 shows BH values of the two BH steels with different pre-deformations tested by tensile experiments. The BH values without pre-deformation were measured as the difference between the two yield stresses of steels with and

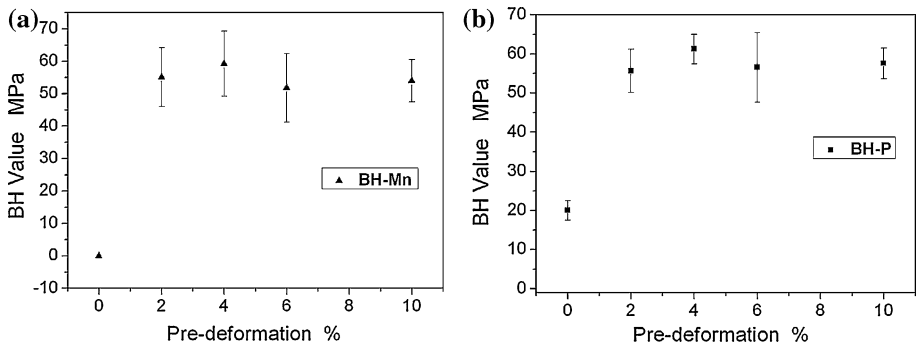

Fig. 8 BH values of BH-Mn (**a**) and BH-P (**b**) steels with different pre-deformations

without baking at 170 °C for 20 min, and the other BH values were the difference between flow stress at the end of pre-deformation and the yield stress after baking.

As shown in Fig. 8, there is no BH value in the BH-Mn steel without pre-deformation, but the BH value is about 20 MPa in the BH-P steel. As is known, BH value is induced by the diffusion of solute C and the pinning of C on dislocations during baking process. So the possible reason of the result is that there is no BH value in the BH-Mn steel without pre-deformation and there is low C concentration (see Table 1) and more importantly very few dislocations (see Fig. 1) in this steel. There are much more dislocations induced by the significant segregation of P in the annealed BH-P steel as shown in Fig. 3 and more solute C as listed in Table 1, so the BH value in BH-P steel without pre-deformation is much higher.

When pre-deformations are added to the BH steels, BH value increases obviously in both BH steels. As shown in Fig. 8, the variation law of BH values in the two BH steels is similar when pre-deformation is more than 2%. Since there is no obvious change of C in BH-Mn steel with different pre-deformations as discussed in "Solute distributions in pre-deformed and baked BH-Mn steel" section, BH-P steel is used as example to discuss the BH phenomenon variation with different pre-deformations. As discussed in "Solute distributions in pre-deformed and baked BH-P steel" section, there are more C clusters in the BH-P steel matrix, and the C concentration decreases with the pre-deformation increases to 2%. Since BH value is induced by the pinning of solute C on dislocations, this 3DAP result is in agreement with the result that the BH value increases obviously when the pre-deformation increases to 2%. As shown in Fig. 8, there is a slight decrease of BH value in both BH steels when pre-deformation increases to 6%, and then BH value changes very little till 10%. The slight decrease of BH value is considered to be a balance process of Cottrell atmosphere formed by solute C and pinned dislocations. It is obvious that at about 4% pre-deformation, BH value is the highest of about 60 MPa. So the 4% pre-deformation makes a critical balance of solute C and pinned dislocations in the test BH steels.

Conclusions

Solute distributions in two kinds of BH steels with different compositions and heat treatments were investigated by 3DAP. BH values of these steels were tested by tensile experiments.

The results indicate that C concentration in the annealed BH-Mn steel is obviously lower than that in the annealed BH-P steel. C distribution changes little with the increase of pre-deformation in BH-Mn steel. In BH-P steel, however, C diffuses during the pre-deformation and baking process, which forms more C clusters and induces the decrease of C concentration in the matrix. The distribution patterns and the maximum separation distance method results prove that the C cluster is just C segregation or C together with P segregation rather than vanadium carbides precipitate. V segregates most obviously at 2% pre-deformation in both BH steels. Mn segregates more obviously in the pre-deformed and baked BH-Mn steel than in annealed one. P segregates in all the BH-P steels with different treatments.

There is no BH phenomenon in BH-Mn steel without pre-deformation because there is very low C concentration and very little dislocations in the steel matrix. The BH value in BH-P steel without pre-deformation is much higher than that in BH-Mn steel. BH values are similar in the two BH steels when pre-deformation is more than 2%. The BH value increases slightly with the pre-deformation increases to 4%, decreases slightly at 6%, and changes very little till 10%. The 4% pre-deformation induces the highest BH values in the two BH steels, and is considered to be the critical pre-deformation in making the balance of Cottrell atmosphere.

Acknowledgements The authors are thankful to VANITEC, National Nature Science foundation of China program under Grant

No. 50934011, and National Basic Research Program of China (973) under Grant No. 2010CB630802 for the project funding.

References

1. Tanioku T, Hoboh Y, Okamoto A, Mizui N (1991) Development of a new bake-hardenable galvannealed sheet steel for automotive exposed panels. In: SAE Technical Paper 910293, Warrendale, pp 303–308
2. Taylor KA, Speer JG (1997) Development of vanadium-alloyed, bake-hardenable sheet steels for hot-dip coated applications. In: 39th MWSP conference proceedings, ISS, vol XXXV, Indianapolis, pp 49–61
3. Hong MH, Cho NH, Kim SI, Kwon O, Lim SH, Moon WJ (2010) Met Mater Int 16:883
4. Waterschoot T, Vandeputte S, De Cooman BC, Houbaert Y (1999) The Influence of P, Si and Mn on the mechanical properties and bake-hardening of Ti-ULC Steels. In: 41st MWSP conference proceedings, ISS, vol XXXVII, Indianapolis, pp 425–433
5. Birol Y (2010) J Mater Sci 45:6727. doi:10.1007/s10853-010-4766-z
6. Milititsky M, Decooman B, Speer J, De Wispelaere N, Akdut N (2006) Metall Mater Trans A 37:2117
7. Wen Y, Su Q, Wuttig M (1998) Interstitial analysis of ultra low carbon and interstitial free steels. In: 39th MWSP conference proceedings, ISS, vol XXXV, pp 271–280
8. De AK, De Blauwe K, Vandeputte S, De Cooman BC (2000) J Alloys Compd 310:405
9. Soenen B, De AK, Vandeputte S, De Cooman BC (2004) Acta Mater 52:3483
10. Al-Shalfan W, Speer JG, Findley K, Matlock DK (2006) Metall Mater Trans A 37A:206
11. Miller MK (2006) J Mater Sci 41:7808. doi:10.1007/s10853-006-0518-5
12. Blavette D, Duval P, Letellier L, Guttmann M (1996) Acta Mater 44:4995
13. Menand A, Cadel E, Pareige C, Blavette D (1999) Ultramicroscopy 78:63
14. Hono K (1999) Acta Mater 47:3127
15. Wilde J, Cerezo A, Smith GDW (2000) Scr Mater 43:39
16. Ping DH, Hono K, Nie JF (2003) Scr Mater 48:1017
17. Oh JC, Ohkubo T, Mukai T, Hono K (2005) Scr Mater 53:675
18. Pereloma EV, Timokhina IB, Miller MK, Hodgson PD (2007) Acta Mater 55:2587
19. Caballero FG, Miller MK, Garcia-Mateo C, Capdevila C, Babu SS (2008) Acta Mater 56:188
20. Yamaguchi Y, Takahashi J, Kawakami K (2009) Ultramicroscopy 109:541
21. Grennan-Heaven N, Cerezo A, Godfrey TJ, Smith GDW (2007) Ultramicroscopy 107:705
22. Rachbauer R, Stergar E, Massl S, Moser M, Mayrhofer PH (2009) Scr Mater 61:725
23. Takahashi J, Tarui T, Kawakami K (2009) Ultramicroscopy 109:193
24. Takahashi J, Kawakami K, Otsuka H, Fujii H (2009) Ultramicroscopy 109:568
25. Liu QD, Liu WQ, Wang ZM, Zhou BX (2008) Acta Metall Sin 44:786 (in Chinese)
26. Wang H, Shi W, He YL, Fu RY, Li L (2011) Acta Metall Sin 3:263 (in Chinese)
27. De AK, Vandeputte S, Cooman BCD (2001) Scr Mater 44:695
28. Zhao JZ, De AK, De Cooman BC (2000) Mater Lett 44:374